particles

MDPI

Article

Hayward–Letelier Black Holes in AdS Spacetime

Arun Kumar [1,2,†], Ashima Sood [3,4,†], Sushant Ghoshtokumar Ghosh [4,5,†] and Aroonkumar Beesham [6,*,†]

1 Institute for Theoretical Physics and Cosmology, Zhejiang University of Technology, Hangzhou 310023, China; arunbidhan@gmail.com
2 Department of Mathematical Sciences, University of Zululand, Private Bag X1001, Kwa-Dlangezwa 3886, South Africa
3 Department of Mathematics, Netaji Subhas University of Technology, New Delhi 110078, India; ashimasood1993@gmail.com
4 Centre for Theoretical Physics, Jamia Millia Islamia, New Delhi 110025, India; sghosh2@jmi.ac.in
5 Astrophysics and Cosmology Research Unit, School of Mathematics, Statistics and Computer Science, University of KwaZulu-Natal, Private Bag 54001, Durban 4000, South Africa
6 Faculty of Natural Sciences, Mangosuthu University of Technology, P.O. Box 12363, Jacobs 4026, South Africa
* Correspondence: abeesham@yahoo.com
† These authors contributed equally to this work.

Abstract: We analyze Hayward black holes (BHs) with a negative cosmological constant surrounded by a cloud of strings, which we designate Hayward–Letelier AdS BHs. These solutions can be obtained by coupling the Einstein equations with nonlinear electrodynamics and the energy–momentum tensor of clouds of strings. We show that these solutions are no longer regular and have a curvature singularity at the center. In turn, we analyze the thermodynamics associated with these BHs by establishing the form of the Smarr formula and the first law of thermodynamics. We derive the expressions for the thermodynamic quantities such as pressure, temperature, heat capacity, Gibbs free energy, and isothermal compressibility. We explore the phase structure of these solutions by analyzing the behavior of the heat capacity and Gibbs free energy. These solutions exhibit a first-order phase transition, similar to van der Waals fluids. We also check the behavior of the thermodynamic quantities near the critical points and calculate the values of the critical exponents. This illustrates a robust analogy between our solutions and van der Waals fluids.

Keywords: Hayward–Letelier black holes; AdS spacetime; negative cosmological spacetime; cloud of strings; nonlinear electrodynamics; thermodynamics quantities; phase structure of solutions

Citation: Kumar, A.; Sood, A.; Ghosh, S.G.; Beesham, A. Hayward–Letelier Black Holes in AdS Spacetime. *Particles* **2024**, *7*, 1017–1037. https://doi.org/10.3390/particles7040062

Academic Editor: Armen Sedrakian

Received: 11 August 2024
Revised: 2 November 2024
Accepted: 16 November 2024
Published: 20 November 2024

1. Introduction

Einstein's general relativity (GR), the most celebrated theory of gravity, opened up a new, enormously vast field of research for astrophysicists by predicting the existence of some mysterious astrophysical objects that are ideal absorbers (absorb everything and emit nothing) of nature. These astonishing compact objects known as black holes (BHs) have a singularity at the center surrounded by the event horizon [1]. The presence of spacetime singularities shows the breakdown of GR, which is believed to be because of ignorance of the quantum mechanical effect in GR. The singularity problem in GR can be dealt with by developing a more fundamental quantum theory of gravitation. In the absence of a quantum theory of gravity, resolving curvature singularities at the level of classical gravity remains open.

Sakharov [2] and Gliner [3] demonstrated that matter can avoid the singularities, i.e., with a de Sitter core, with the equation of state $p = -\rho$. This development led Bardeen [4] to propose a black solution without a singularity at its center. He termed these solutions regular BHs because the spacetime is well-behaved everywhere, including at the center $r = 0$. Beato and Garcia [5] obtained the exact Bardeen solution. Bronnikov [6,7] made a fascinating observation regarding regular black holes. This observation highlights that

for the regularity of black holes, the nonlinear electrodynamics (NED) charge must be a magnetic monopole. Since then, there has been an intense study of regular BHs that are exact solutions of GR minimally coupled to NED [8–19].

Hayward [20] proposed a new regular spacetime, which can be described by the following spherically symmetric metric

$$ds^2 = -\left(1 - \frac{2mr^2}{r^3 + 2l^2m}\right)dt^2 + \frac{1}{\left(1 - \frac{2mr^2}{r^3+2l^2m}\right)}dr^2 + r^2(d\theta^2 + sin^2\theta d\phi^2). \quad (1)$$

Solution (1) is characterized by the BH mass m and the fundamental length l. At a large distance, this solution behaves like Schwarzschild's solution, while at a small distance, it behaves like an AdS vacuum solution. The Hayward solution is straightforward for analysis as it can be obtained by minimally coupling GR with NED (with magnetic charge g, where the charge g is defined by $g^3 = 2\,mL^2$), and hence, has received significant attention in the last two decades [21–32].

BH thermodynamics is a fascinating subject that combines gravity with quantum mechanics semi-classically and indicates that it is possible to relate BH physics with other areas of fields through the AdS/CFT correspondence [33–35]. The story of BH thermodynamics started with identifying the surface gravity and area of the event horizon as the BH temperature and entropy, respectively, [36,37]. Later, Bardeen et al. [38] gave a set of four laws governing BH thermodynamics. The pioneering work by Hawking and Page [39], in which they demonstrated that BHs can undergo a phase transition to thermal radiation in AdS space, showed that the BHs possess rich phase structures analogous to ordinary thermodynamic systems. In AdS spacetime, where the negative cosmological constant is identified as positive pressure [40,41], charged BHs show a van der Waals-like phase transition between small and large BHs [42–44], which is analogous to the liquid–gas phase transition of a van der Waal's fluid. In contrast, some BHs exhibit re-entrant phase transition [42,45], triple points [46], and heat engines [47].

This article aims to obtain a spherically symmetric Hayward BH solution surrounded by a cloud of strings (CS) in AdS spacetime (Hayward–Letelier AdS BH) and to find the effects of CS on the geometric as well as thermodynamic aspects of Hayward BHs. The consideration of the BH solution surrounded by CS is motivated by the argument that the Universe's fundamental building blocks may be extended objects instead of point objects. In that case, the one-dimensional string can be the most natural candidate [48]. Letelier [49] was the first to study BHs surrounded by CS. The event horizon for the classical Schwarzschild metric in the background of a CS has a modified radius of $r_H = 2M/(1-a)$, where a is a string cloud parameter [49]. This enlargement of the Schwarzschild radius by the factor $(1-a)^{-1}$ may have several astrophysical consequences, such as the formation of wormholes. In recent times, a lot of attention has been given to BHs with CS background [50–56]. The study of Einstein's equations coupled with CS in GR and modified theories may be significant.

The rest of the work is organized as follows: Section 2 discusses the geometric aspects of Hayward–Letelier BHs in AdS spacetime. Section 3 is dedicated to deriving and discussing various thermodynamic quantities. Section 4 discusses the thermodynamic stability and critical points of BHs. In contrast, in Section 5, we examine the behavior of thermodynamic quantities near the critical point and determine the value of critical exponents. Finally, we conclude the paper in Section 6.

2. Hayward–Letelier Solution in AdS Spacetime

Here, we intend to obtain a Hayward–Letelier BH in AdS spacetime. The action reads

$$S = \int d^4x\sqrt{-g}\left[R + 6L^{-2} + L_{NED}\right] + S_M, \quad (2)$$

where R is the curvature scalar, L is positive AdS radius related to the cosmological constant Λ through the relation $\Lambda = -3/L^2$, and L_{NED} is the nonlinear Lagrangian of electromagnetic theory. The Lagrangian is a nonlinear function of the electromagnetic scalar $\mathcal{F} = F^{\mu\nu}F_{\mu\nu}$, where $F_{\mu\nu} = \partial_\mu A_\nu - \partial_\nu A_\mu$ is the Maxwell–Faraday tensor for gauge potential A_μ. S_M is the Nambu–Goto action of the cloud of strings. The Lagrangian for the Hayward solution that we are interested in is given as

$$L_{NED}(\mathcal{F}) = \frac{12\bar{\mu}(g^2\mathcal{F}/2)^{\frac{3}{2}}}{g^3\left[1+(\sqrt{g^2\mathcal{F}/2})^{\frac{3}{2}}\right]^2}, \tag{3}$$

where $\bar{\mu}$ is a positive constant and g is the magnetic monopole charge. The action S_M reads [49,56]

$$S_M = \mathcal{M}\int_\Sigma \sqrt{-\gamma}\, d\lambda^0 d\lambda^1 = \mathcal{M}\int_\Sigma \left[-\frac{1}{2}\Sigma_{\mu\nu}\Sigma^{\mu\nu}\right]^{\frac{1}{2}} d\lambda^0 d\lambda^1, \tag{4}$$

where spacelike and timelike parameters parameterize the world sheet [48] represented by λ^0 and λ^1, and $\mathcal{M}$ is a dimensionless positive constant that characterizes each string. The quantity γ is the determinant of γ_{ab} given by

$$\gamma_{ab} = g_{\mu\nu}\frac{\partial x^\mu}{\partial\lambda^a}\frac{\partial x^\nu}{\partial\lambda^b}. \tag{5}$$

The movement of a string in time sweeps out an area in two dimensions, which is termed as its [48] world sheet Σ and has associated with it a bivector given by [49]

$$\Sigma^{\mu\nu} = \epsilon^{ab}\frac{\partial x^\mu}{\partial\lambda^a}\frac{\partial x^\nu}{\partial\lambda^a}, \tag{6}$$

where ϵ^{ab} is the Levi–Civita tensor in two dimensions, which is anti-symmetric in the indices a and b given by $\epsilon^{01} = -\epsilon^{10} = 1$. Variation of action (4) with respect to metric $g_{\mu\nu}$ leads to following equation of motions

$$R_{\mu\nu} - \frac{1}{2}g_{\mu\nu}R - 3L^{-2}g_{\mu\nu} = \kappa^2(T^{NED}_{\mu\nu} + T^{\text{cs}}_{\mu\nu}). \tag{7}$$

The tensor $F_{\mu\nu}$ obeys

$$\nabla_\mu\left(\frac{\partial L_{NED}(\mathcal{F})}{\partial\mathcal{F}}F^{\mu\nu}\right) = 0 \tag{8}$$

and the Bianchi identities

$$\nabla_\mu({}^*F^{\mu\nu}) = 0, \tag{9}$$

where $*$ denotes the Hodge dual. We consider a spherically symmetric metric ansatz

$$ds^2 = -f(r)dt^2 + \frac{1}{f(r)}dr^2 + r^2\left(d\theta^2 + \sin^2\theta d\phi^2\right). \tag{10}$$

For a spherically symmetric spacetime that is only magnetically charged, the only nonzero component of $F_{\mu\nu}$ is as in [6] (In [57], the authors explicitly show how the nonzero components are obtained for a spherically symmetric electromagnetic field).

$$F_{\theta\phi} = g\sin\theta, \tag{11}$$

and the scalar $\mathcal{F}$ is

$$\mathcal{F} = \frac{2g^2}{r^4}. \tag{12}$$

The energy–momentum tensor of NED reads

$$T_{\mu\nu}^{NED} = 2\left(\frac{\partial L_{NED}(\mathcal{F})}{\partial \mathcal{F}}\mathcal{F}_{\mu\sigma}\mathcal{F}_{\nu}^{\sigma} - \frac{1}{4}g_{\mu\nu}L_{NED}(\mathcal{F})\right), \tag{13}$$

and that of the cloud of strings as [49,53,56]

$$T_{\mu\nu}^{\text{cs}} = \frac{\rho\Sigma_{\mu\sigma}\Sigma_{\nu}^{\sigma}}{\sqrt{-\gamma}} \tag{14}$$

with ρ, and $\rho/\sqrt{-\gamma}$ are the proper density and gauge invariant density of the cloud of strings, respectively. The strings are characterized by a surface-forming bivector $\Sigma_{\mu\nu}$, and the conditions for being surface-forming are $\Sigma^{\mu[\alpha}\Sigma^{\beta\gamma]} = 0$ and $\nabla_{\mu}\Sigma^{\mu[\alpha}\Sigma^{\beta\gamma]} = 0$, where the square brackets denote antisymmetrization. These equations, along with Equation (6), lead to the useful identity

$$\Sigma^{\mu\sigma}\Sigma_{\sigma\tau}\Sigma^{\tau\nu} = \gamma\Sigma^{\nu\mu}, \tag{15}$$

which will be employed in subsequent calculations. By applying conservation of the energy–momentum condition, $T_{;\mu}^{\mu\nu} = 0$, and using Equation (15), we performed some tensor calculus as given in [53,54] to obtain the following condition

$$\nabla_{\mu}(\rho\Sigma^{\mu\sigma})\Sigma_{\sigma}^{\nu} = 0 \tag{16}$$

which, on using the coordinate system adapted to the surface parameterization, results in in [53,54,56]

$$\partial_{\mu}(\sqrt{-g}\rho\Sigma^{\mu\sigma}) = 0 \tag{17}$$

where ρ and $\Sigma^{\mu\nu}$ depend only on r, as we are looking for static, spherically symmetric solutions. The only non-zero component of the bivector Σ is $\Sigma^{tr} = -\Sigma^{rt}$. Consequently, $T_t^t = T_r^r = -\rho|\Sigma^{tr}|$, and from Equation (17), we obtain $\partial_r(r^2T_t^t) = 0$ and, hence, we obtain the energy–momentum tensor for the cloud of strings [53,54,56]

$$(T_{\mu}^{\nu})^{\text{cs}} = \text{diag}\left[\frac{a}{r^2}, \frac{a}{r^2}, 0, 0\right] \tag{18}$$

Solving the Einstein equations, on using Equations (3), (7), (12), (13), and (18), we obtain the metric function

$$f(r) = 1 - \frac{2Mr^2}{g^3 + r^3} - a + \frac{r^2}{L^2}, \tag{19}$$

where a is the cloud of strings parameter, and M is the constant of integration interpreted as the mass of the black hole found to be equal to $\bar{\mu}$. In the limiting case, $a \to 0$, we find the Hayward–AdS solution [21], and for $g \to 0$, the solution (19) reduces to the Schwarzschild–AdS BH surrounded by a cloud of strings [58].

In order to locate the horizons, it is necessary to solve the equation $f(r) = 0$. Unfortunately, obtaining analytical expressions for the horizon radius is not feasible. Therefore, we employ numerical analysis to examine the horizon structure. This involves plotting the metric function $f(r)$ against the radial coordinate r in Figure 1. By doing so, we can determine up to two horizons, which are contingent upon the values of several parameters (g, a, L). To verify curvature singularities, it suffices to examine the Kretschmann scalar, denoted as $K = R^{\mu\nu\alpha\beta}R_{\mu\nu\alpha\beta}$, where $R^{\mu\nu\alpha\beta}$ represents the Riemann tensor, which reads

$$
\begin{aligned}
K \;=\; & \frac{4a}{r^4}\left(a+\frac{4Mr^2}{r^3+g^3}-\frac{2r^2}{L^2}\right)+\frac{16M}{r^3+g^3}\left(\frac{M}{r^3+g^3}-\frac{1}{L^2}\right)+\frac{4}{L^4} \\
& +4\left(-\frac{4M}{r^3+g^3}+\frac{6Mr^3}{(r^3+g^3)^2}+\frac{2}{L^2}\right)^2 \\
& +\left(-\frac{4M}{r^3+g^3}+\frac{36Mr^3}{(r^3+g^3)^2}-\frac{36Mr^6}{(r^3+g^3)^3}+\frac{2}{L^2}\right)^2
\end{aligned} \tag{20}
$$

Because we included the parameter a of the cloud of strings, the Hayward BH loses its regularity, and the Hayward–Letelier AdS BH has a curvature-singularity at the origin.

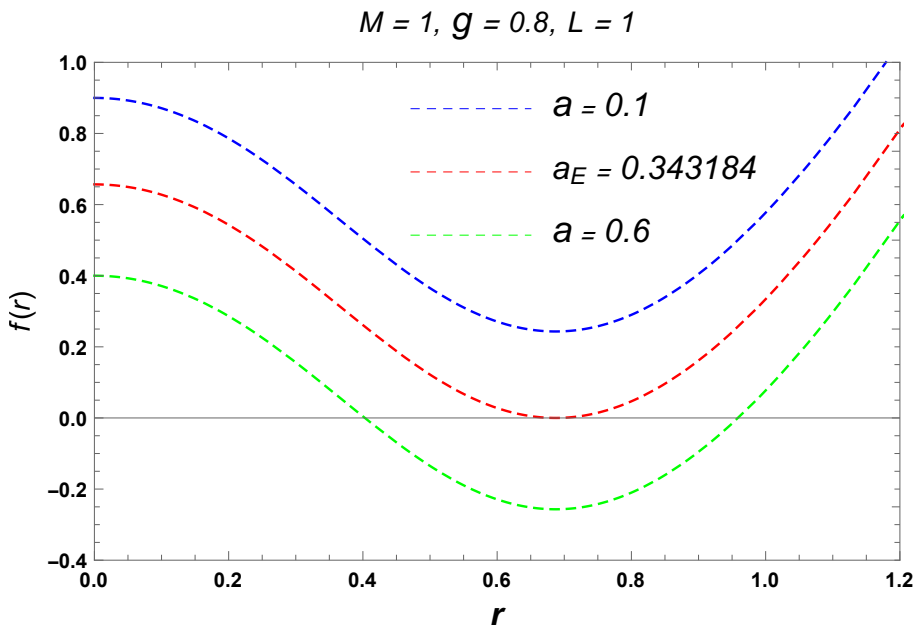

Figure 1. Graphical representation of $f(r)$ with respect to the radial coordinate with different values of a and fixed $g = 0.8$, $M = 1$, and $L = 1$.

3. Thermodynamics

The investigation of BH thermodynamics is a fascinating area of study. In the following section, we inquire into BH thermodynamics. John Wheeler [59,60] was the first to notice that for any system consisting of a BH to follow the non-decreasing entropy law, it is necessary to assign temperature and entropy to the BH. Based on this assertion, we can conclude that a body while falling into a black hole transfers its entropy alongside its mass, angular momentum, and charge. Later, Bekenstein and Hawking made a breakthrough in the thermodynamic aspect of BHs, by relating the temperature and entropy of BHs at the event horizon, respectively, with the surface gravity and the area of the event horizon [36–38,61]. The temperature of a BH is related to its surface gravity by $T_\kappa = \kappa/2\pi$ [62], where the surface gravity κ is given by $\kappa = f'(r)/2|_{r=r_+}$, where r_+ is the event horizon radius. Using the above relation, we obtain the temperature for the Hayward–Letelier AdS BH as

$$
T_k = \frac{1}{4\pi r_+(r_+^3+g^3)}\left[r_+^3\left(1-a+\frac{3r_+^2}{L^2}\right)-2(1-a)g^3\right]. \tag{21}
$$

In extended phase space thermodynamics, the negative cosmological constant Λ is treated as a thermodynamic pressure (P) as:

$$
P = -\frac{\Lambda}{8\pi} \equiv \frac{3}{8\pi L^2} \tag{22}
$$

By incorporating the cosmological constant as a thermodynamic pressure and interpreting the BH mass as enthalpy, extended phase space thermodynamics provides a more comprehensive understanding of BH thermodynamics. As our black hole solution exhibits two horizons, there must be different temperatures associated with these horizons. Hence, theoretically, it is not possible to attain the thermal equilibrium. Here, we are taking into consideration that the event horizon can attain a quasi-equilibrium with the surroundings and the inner horizon remains isolated; thus, we can use the first law of black hole thermodynamics to describe the thermodynamic properties. The first law of BH thermodynamics for a charged and static BH in extended phase space becomes modified by the inclusion of charge and cosmological constant along with their conjugates and has the following form [42]

$$dM = T_H dS + \Phi dg + V dP, \tag{23}$$

where M is the enthalpy of the system, Φ is the magnetic charge potential, and S is the entropy of the system, which can be expressed in terms of the horizon area of a BH as [37]

$$S = \frac{A}{4} = \pi r_+^2, \tag{24}$$

where A is the area of the BH horizon. By using the first law of BH thermodynamics given in Equation (23), one can derive the temperature and magnetic potential as follows:

$$T_H = \frac{\partial M}{\partial S}, \text{ and } \Phi = \frac{\partial M}{\partial g}. \tag{25}$$

By solving for $f(r_+) = 0$, we obtain the mass M of the BH as

$$M = \frac{\left(g^3 + r_+^3\right)\left(3(1-a) + \frac{3r_+^2}{L^2}\right)}{6r_+^2}. \tag{26}$$

Using Equation (26) in Equation (25) leads to the following BH temperature expression

$$T_H = \frac{r_+^3\left(3(1-a) + \frac{3r_+^2}{L^2}\right) - 2(1-a)g^3}{4\pi r_+^4}. \tag{27}$$

It is intriguing that the temperature determined through surface gravity, denoted as T_κ, does not align with the temperature obtained from the first law, represented as T_H. This discrepancy arises because of the invalidity of the first law, as presented in Equation (23), within theories coupled to NED [63–65]. The Lagrangian density of NED relies explicitly on the mass, necessitating a modification in the first law [66,67].

$$d\mathcal{M} = dM\left(1 - \int_{r_+}^{\infty} r^2 \frac{\partial T_0^0}{\partial M} dr\right) = W(r_+, g) dM, \tag{28}$$

where $W(r_+, g)$ is the correction factor, given by

$$W(r_+, g) = \left(1 - \int_{r_+}^{\infty} r^2 \frac{\partial T_0^0}{\partial M} dr\right), \tag{29}$$

and T_0^0 is one of the components of the stress–energy tensor. The correction factor, $W(r_+, g)$, correlates the old and new thermodynamic quantities.

The two temperatures, T_κ and T_H, are related to each other by

$$T_k = W(r_+, g)T_H = W(r_+, q)\frac{\partial M}{\partial S} = \frac{1}{4\pi r_+(r_+^3 + g^3)}\left(r_+^3(1 - a + \frac{3r_+^2}{L^2}) - 2(1-a)g^3\right), \tag{30}$$

with $W(r_+, g) = r_+^3/r_+^3 + g^3$.

As depicted in Figures 2 and 3, the temperature exhibits a varying pattern with the entropy S, and displays local maxima and minima. This behavior confirms the occurrence of phase transitions between different stages of BHs. The temperature reaches zero at a specific entropy value, revealing an extremal BH. The extremal BH's entropy allows us to determine its corresponding radius, which can also be calculated from the metric function. The extremal BH radius corresponds to where the metric function $f(r)$ reaches its minimum, signifying that the derivative of the metric function at that point is zero. The temperature expressions for the Hayward–AdS and Schwarzschild–Letelier–AdS BHs, respectively, are as shown in the figures.

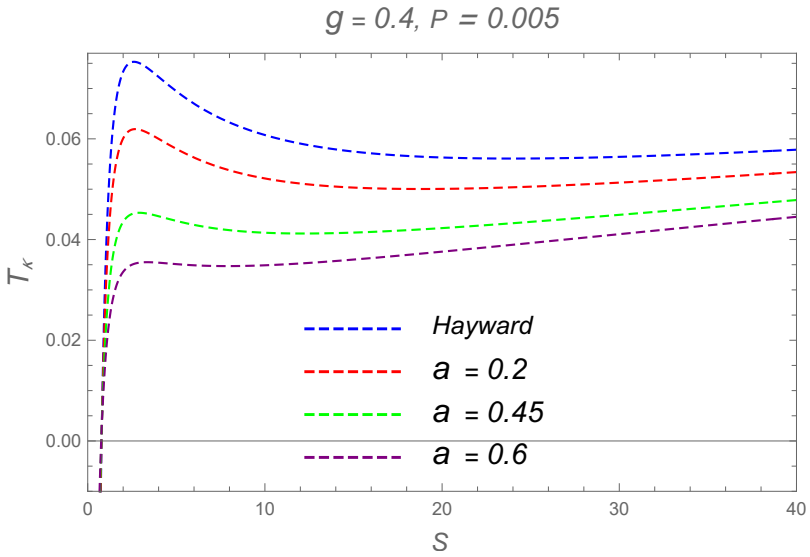

Figure 2. Graphical representation depicting the temperature associated with the Hayward–Schwarzschild–Letelier–AdS solution (21) for varying values of a.

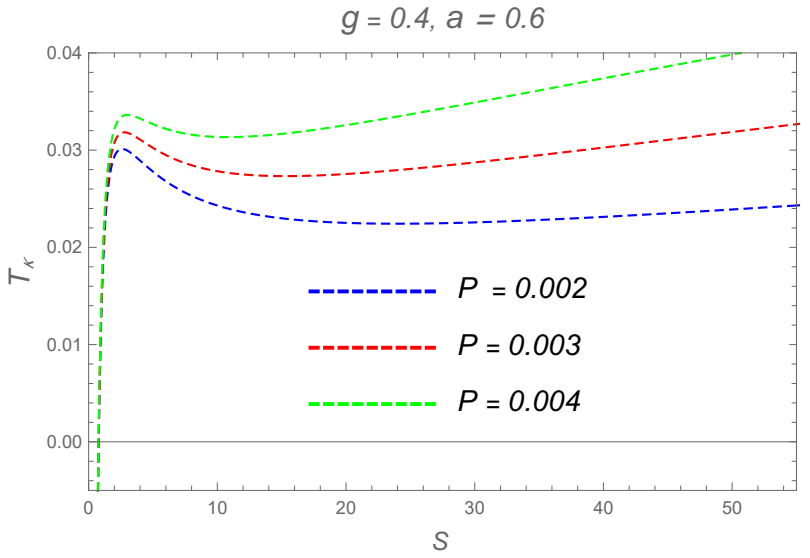

Figure 3. Graphical representation depicting the temperature associated with the Hayward–Schwarzschild–Letelier–AdS solution (21) for varying values of P.

$$T_{kH} = \frac{r_+^3\left(3+\frac{3r_+^2}{L^2}\right)-2g^3}{4\pi r_+^4}, \tag{31}$$

$$T_{kL} = \frac{r_+^3\left(3(1-a)+\frac{3r_+^2}{L^2}\right)}{4\pi r_+^4}. \tag{32}$$

Next, we want to derive the Smarr formula, which establishes a relation between the mass and the other parameters. We can obtain the Smarr formula by using the properties of the homogeneous function [68]. To do so, first, we write the mass of the BH in terms of entropy as

$$M(S,g,a,\Lambda) = \frac{1}{6S}(3\pi(1-a)-\Lambda S)\left(g^3+\frac{S^{3/2}}{\pi^{3/2}}\right). \tag{33}$$

To find out the degree of homogeneity of the mass, we rewrite it in the given form

$$M(l^hS,l^bg,l^ca,l^d\Lambda) = \frac{1}{6l^hS}\left(3\pi(1-l^ca)-l^{h+d}\Lambda S\right)\left(l^{3b}g^3+l^{3h/2}\frac{S^{3/2}}{\pi^{3/2}}\right). \tag{34}$$

By assuming $b = h/2$, $d = -h$, $c = 0$, and $h = 1$, we isolate l, and Equation (34) becomes

$$M(l^hS,l^bg,l^ca,l^d\Lambda) = \frac{1}{6S}\sqrt{l}(3\pi(1-a)-\Lambda S)\left(g^3+\frac{S^{3/2}}{\pi^{3/2}}\right). \tag{35}$$

From Equation (35), it can be seen clearly that the mass is a homogeneous function with a degree of homogeneity $n = 1/2$ [68].

According to Euler's identity, a homogeneous function with degree n satisfies the following relation [68]

$$n.f(x_1,x_2\ldots x_m) = a_1x_1\frac{\partial f}{\partial x_1}+a_2x_2\frac{\partial f}{\partial x_2}+a_3x_3\frac{\partial f}{\partial x_3}+\ldots+a_mx_m\frac{\partial f}{\partial x_m}. \tag{36}$$

Using the above relation, we obtain the Smarr formula for our BH solution as

$$\frac{1}{2}M(S,g,a,\Lambda) = T_HS+\frac{1}{2}\Phi g-A_\Lambda\Lambda, \tag{37}$$

where T_H and Φ are given by (25), and A_Λ is

$$A_\Lambda = \frac{\partial M}{\partial\Lambda}. \tag{38}$$

By using Equation (28) and the Smarr formula (37), we can write the complete first law for BHs with NED as

$$W(S,g)dM = T_kdS+W(S,g)\Phi dg+W(S,g)A_\Lambda d\Lambda. \tag{39}$$

As we know, for BHs obtained from NED sources, the Lagrangian depends explicitly on some parameters, such as charge and mass, and thus, the fluctuations in the matter sector can be problematic. However, the modified first law given in Equation (39) shows that changes in the geometry sector can compensate for the fluctuations in the matter sector.

4. Themodynamic Stability and Critical Points

In this section, we explore the thermodynamic stability and phase structure of the BHs through an analysis of the behavior of the heat capacity, Gibbs free energy, and isothermal compressibility, and also discuss the derivatives of the solution to find the critical points. According to classical thermodynamics, a thermodynamic system having $C_V \geq C_P \geq 0$ and $k_T \geq k_S \geq 0$ is thermodynamically stable. Here, C_V and C_P are the specific heat at constant volume and pressure, respectively, and k_T and k_S are the isothermal and isentropic compressibilities, respectively, [69]. The specific heat at constant pressure and isothermal compressibility at constant temperature are given by [70]

$$C_P = T_k \frac{\partial S}{\partial T_k}\bigg|_P, \tag{40}$$

$$k_T = -\frac{1}{V}\frac{\partial V}{\partial P}\bigg|_T. \tag{41}$$

Using Equations (21) and (24) in Equation (40), we derive the following specific heat at constant pressure

$$C_P = \frac{2S\left(\pi^{3/2}g^3 + S^{3/2}\right)\left[S^{3/2}(1-a+\frac{3S}{L^2}) - 2(1-a)\pi^{3/2}g^3\right]}{2g^3\pi^{3/2}\left[\pi^{3/2}g^3 + S^{3/2}\left(5(1-a)+\frac{6S}{L^2}\right)\right] - S^3(1-a-\frac{3S}{L^2})} \tag{42}$$

If we use Equation (27) instead of Equation (21), we obtain

$$\bar{C}_P = \frac{2S\left[S^{3/2}(1-a+\frac{3S}{L^2}) - 2(1-a)\pi^{3/2}g^3\right]}{8(1-a)\pi^{3/2}g^3 - S^3(1-a-\frac{3S}{L^2})}, \tag{43}$$

which is not equal to the heat capacity in Equation (42); however, both heat capacities are connected through the relation given below

$$C_P = W(S,g)\frac{\partial T_H}{\partial T_k}\bar{C}_P. \tag{44}$$

The heat capacity of the Hayward–AdS and Schwarzschild–Letelier–AdS solutions are

$$C_{PH} = \frac{2S\left(\pi^{3/2}g^3 + S^{3/2}\right)\left[S^{3/2}(1+\frac{3S}{L^2}) - 2\pi^{3/2}g^3\right]}{2g^3\pi^{3/2}\left[\pi^{3/2}g^3 + S^{3/2}\left(5+\frac{6S}{L^2}\right)\right] - S^3(1-\frac{3S}{L^2})}, \tag{45}$$

$$C_{PL} = -\frac{2S\left(1-a+\frac{3S}{L^2}\right)}{(1-a-\frac{3S}{L^2})}. \tag{46}$$

Figures 4 and 5 depict the graphical behavior of the specific heat of the solution (19) vs. its entropy. There exist two regions with both positive and negative values for C_P, where the solution is thermodynamically stable and unstable for some values of entropy, respectively. Interestingly, for the range of small values of entropy, the specific heat, as well as the temperature, are negative, and, therefore, this range is nonphysical. Hence, we can conclude that the BH solution exhibits two phase transition points corresponding to maxima and minima of the temperature, where C_P flips its sign from positive to negative or negative to positive such that small and large BHs are stable with $C_P > 0$, whereas the intermediate BHs with $C_P < 0$ are thermodynamically unstable.

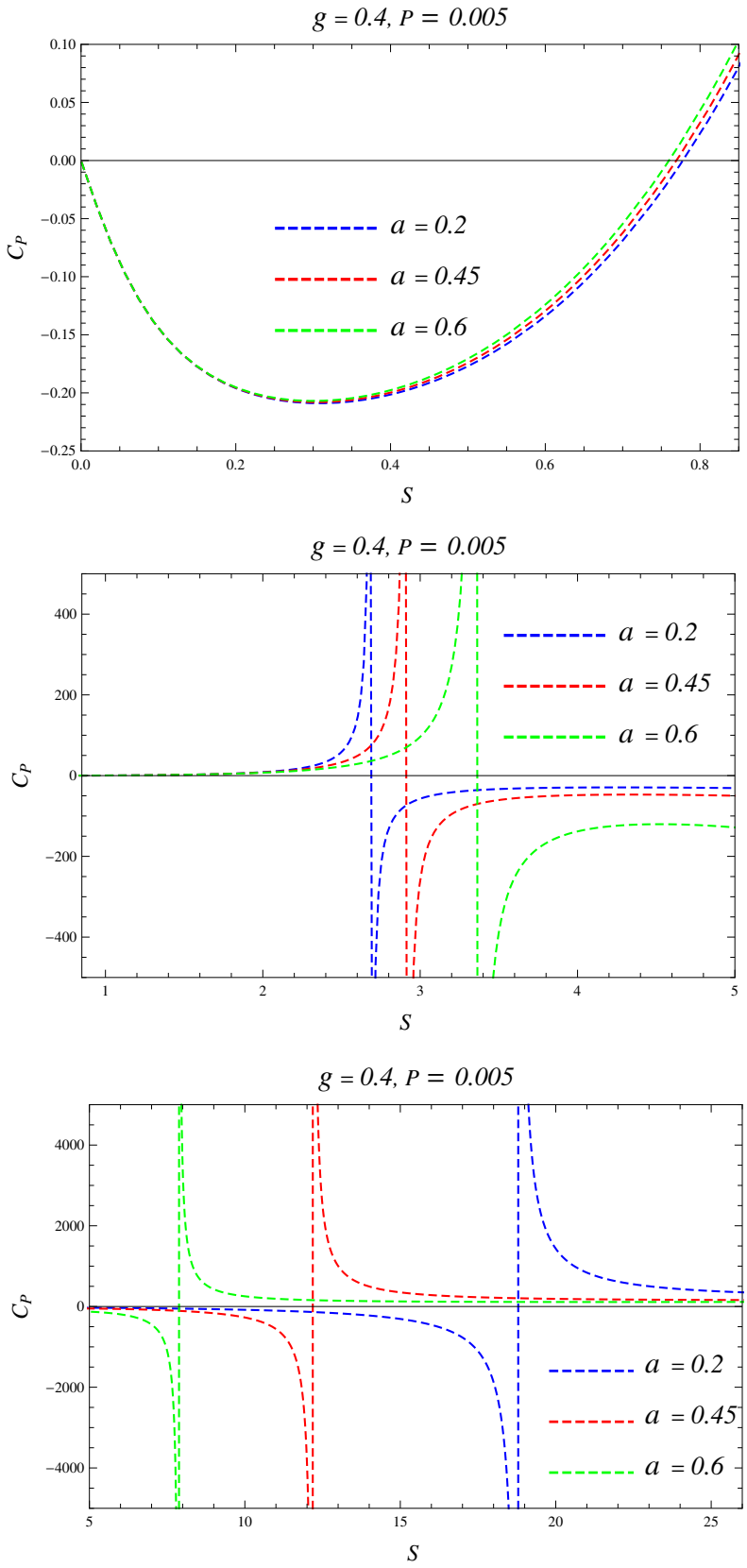

Figure 4. Graphical representation of heat capacity at constant pressure corresponding to the Hayward–Schwarzschild–Letelier–AdS solution (19) by considering $g = 0.4$, $p = 0.005$, and varying values of a and S from left to right.

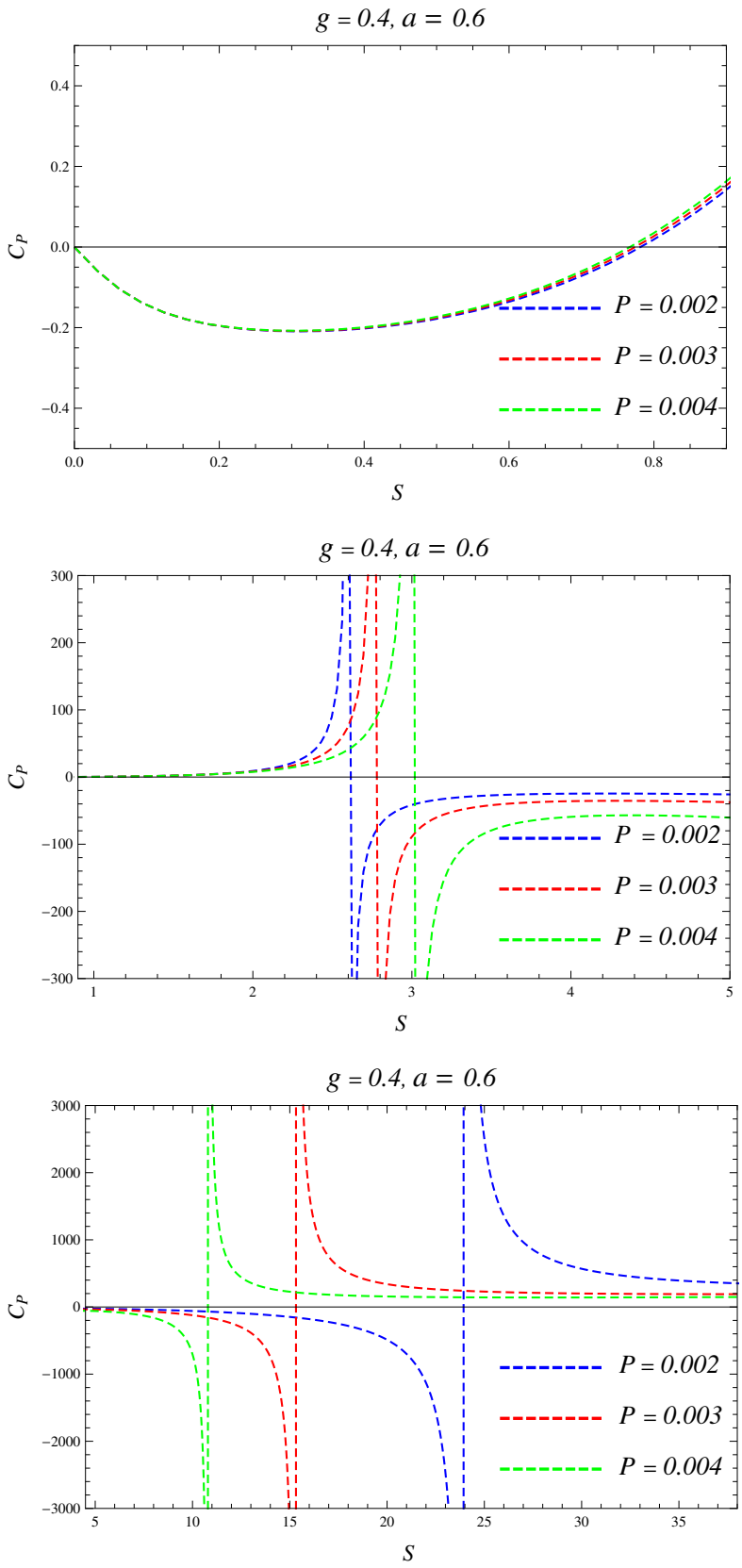

Figure 5. Graphical representation of Heat capacity at constant pressure associated with the Hayward-Schwarzschild–Letelier–AdS solution (19) with $g = 0.4$, $a = 0.6$, and varying values of P and S from left to right.

Next, we want to explore the critical behavior of the solution through the equation of state. We use the modified first law (39) to obtain the thermodynamic volume which reads

$$V = \frac{\partial \mathcal{M}}{\partial P} = \frac{4\pi r_+^3}{3}. \tag{47}$$

Now, by using Equations (21) and (47), the equation of state $P(T, V)$ can be obtained as

$$P(T,V) = \frac{8\pi g^3\left(1 - a + \sqrt[3]{6\pi}T\sqrt[3]{V}\right) - 3V\left(1 - a - 2\sqrt[3]{6\pi^2 V}T\right)}{6\sqrt[3]{36\pi}V^{5/3}}. \tag{48}$$

The pressure for the Hayward–AdS and Schwarzschild–Letelier–AdS solutions are

$$P_H(T,V) = \frac{8\pi g^3\left(1 + \sqrt[3]{6\pi}T\sqrt[3]{V}\right) - 3V\left(1 - 2\sqrt[3]{6\pi^2 V}T\right)}{6\sqrt[3]{36\pi}V^{5/3}}, \tag{49}$$

$$P_L(T,V) = \frac{-3\left(1 - a - 2\sqrt[3]{6\pi^2 V}T\right)}{6\sqrt[3]{36\pi V^2}}. \tag{50}$$

To find the critical points, we use the conditions [71–73]

$$\left(\frac{\partial P}{\partial V}\right)_T = 0, \text{ and } \left(\frac{\partial^2 P}{\partial V^2}\right)_T = 0, \tag{51}$$

which results in the following critical values of pressure, temperature, and volume

$$P_c = \frac{3\left(3+\sqrt{6}\right)(1-a)}{16\,2^{2/3}\pi g^2\left(7+3\sqrt{6}\right)^{5/3}}, \quad T_c = \frac{5^{2/3}(1-a)}{4\pi g\sqrt[3]{118+48\sqrt{6}}},$$
$$V_c = \frac{8}{3}\pi g^3\left(7+3\sqrt{6}\right). \tag{52}$$

The critical points for Hayward–AdS BHs are

$$P_{Hc} = \frac{3\left(3+\sqrt{6}\right)}{16\,2^{2/3}\pi g^2\left(7+3\sqrt{6}\right)^{5/3}}, \quad T_{Hc} = \frac{5^{2/3}}{4\pi g\sqrt[3]{118+48\sqrt{6}}},$$
$$V_{Hc} = \frac{8}{3}\pi g^3\left(7+3\sqrt{6}\right), \tag{53}$$

however, Schwarzschild–Letelier–AdS BHs do not show critical behavior.

In Figure 6, we depict the isotherm on the $P - V$ diagram, corresponding to three different cases, $T < T_c$, $T > T_c$, and $T = T_c$, where T_c is the critical temperature to find the for $T > T_c$, our system behaves like an ideal gas as the pressure monotonically decreases with increasing volume. Conversely, for $T < T_c$, the system shows oscillating behavior, signifying the van der Waals-like phase transition between small (high pressure) and large (low pressure) BHs.

Now, we want to discuss a very important thermodynamic quantity called the compressibility factor, Z, which tells us about the deviation of a thermodynamic system from an ideal gas. The compressibility factor is defined as [69]

$$Z = \frac{PV}{T}. \tag{54}$$

By using the equation of state (48), we obtain the compressibility factor Z as a function of T and V as

$$Z(T,V) = \frac{8\pi g^3\left(1-a+\sqrt[3]{6\pi^2 VT}\right)-3V\left(1-a-2\sqrt[3]{6\pi^2 VT}\right)}{6\sqrt[3]{36\pi V^2 T}}. \tag{55}$$

In the limiting cases $a = 0$ and $g = 0$, we find the compressibility factor of the Hayward–AdS and Schwarzschild–Letelier–AdS BHs, respectively, as

$$Z_H(T,V) = \frac{8\pi g^3\left(1+\sqrt[3]{6\pi^2 VT}\right)-3V\left(1-2\sqrt[3]{6\pi^2 VT}\right)}{6\sqrt[3]{36\pi V^2 T}}, \tag{56}$$

$$Z_L(T,V) = -\frac{\sqrt[3]{V}\left(1-a-2\sqrt[3]{6\pi^2 VT}\right)}{2\sqrt[3]{36\pi T}}. \tag{57}$$

Figure 7 shows the behavior of Z against pressure for different values of temperature. The compressibility factor for our system shows a divergence for small values of pressure. It then decreases as we increase the pressure to reach minima, and then it starts increasing again as we further increase the pressure. We can easily see the deviation of the compressibility factor of our system from the ideal gas for which $Z = 1$. We also calculate the compressibility factor at the critical point, which is $Z_c \approx 1.2345$, which is more than thrice that of a van der Waals fluid ($Z_c = 0.375$ [72]).

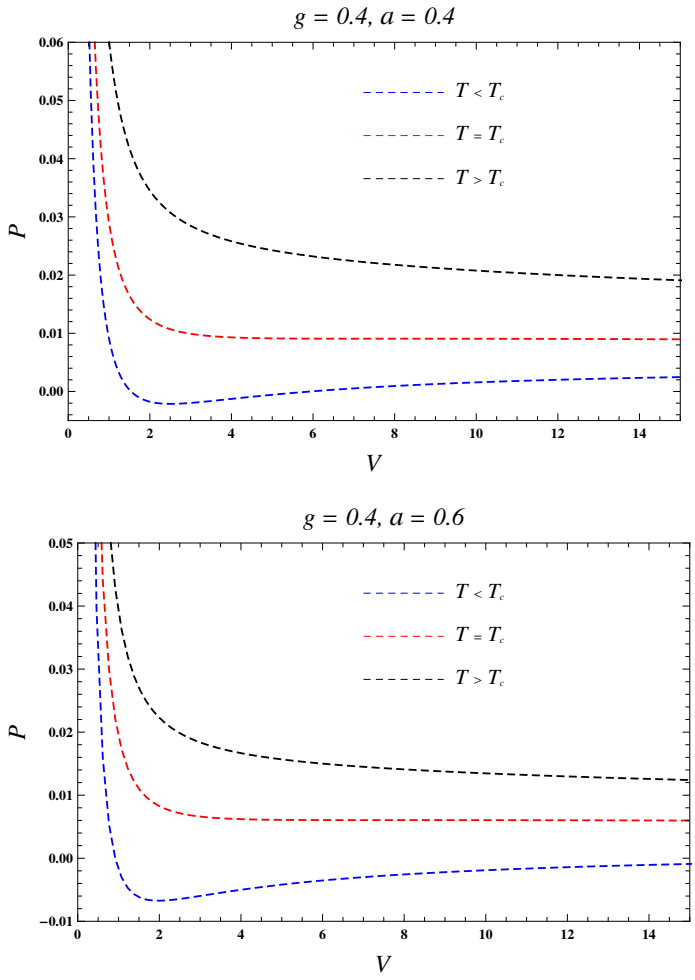

Figure 6. Graphic representation of the $P - V$ behavior of the Hayward–Schwarzschild–Letelier–AdS solution (19) with $T_c = 0.056513$ (**Top**) and $T_c = 0.037675$ (**Bottom**).

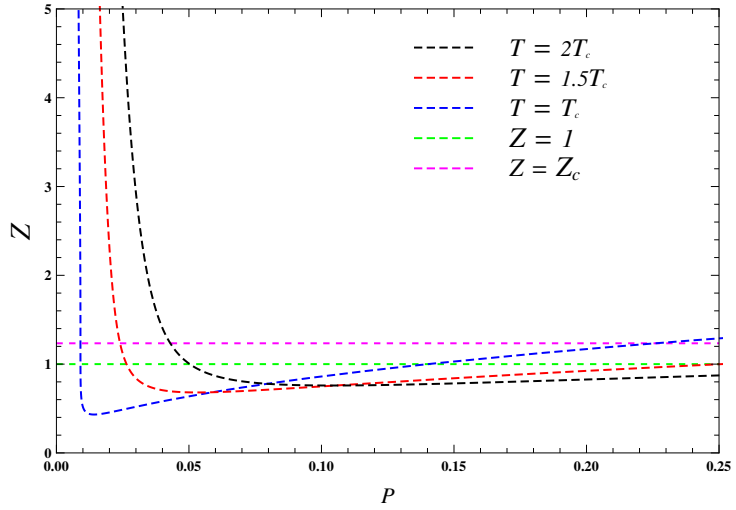

Figure 7. Compressibility factor for Hayward–Schwarzschild–Letelier-AdS solution in terms of the ratio P/P_c to $g = 0.4$, $a = 0.4$, and $T_c = 0.0565133$.

A microscopic analysis of the compressibility factor leads to information about the interaction of molecules of a fluid [66,74]. So, it is very interesting to carry out this analysis of BHs by considering BHs to be made of some virtual molecules. According to Wei and Liu [75], it is possible to analyze a BH microscopically through the idea of virtual molecules. Hence, we would like to do the microscopic analysis through the number density of virtual micro-molecules of the BH, i.e.,

$$n = \frac{1}{v} = \frac{1}{2l_p^2 r_+}, \tag{58}$$

where v, and $l_p = \sqrt{\hbar G/c^3}$ are the specific volume of the BH and the Planck length, respectively. Here, we are taking natural units, $l_p = 1$ and $n = 1/v = 1/2r_+$. Noticeably, the specific volume is linear with the event horizon radius r_+. So, we rewrite temperature in terms of the number density, which reads

$$T(n) = \frac{(1-a)n^2\left(1-16g^3n^3\right)+2\pi P}{2\pi n(8g^3n^3+1)}. \tag{59}$$

By keeping $a = 0$, and $g = 0$, we can obtain the temperature of Hayward–AdS and Schwarz-schild–Letelier–AdS BHs, respectively, as

$$T_H(n) = \frac{n^2\left(1-16g^3n^3\right)+2\pi P}{2\pi n(8g^3n^3+1)}, \tag{60}$$

$$T_L(n) = \frac{2\pi P+(1-a)n^2}{2\pi n}. \tag{61}$$

The behavior of temperature against number density for different values of pressure is depicted in Figure 8.

Next, we want to check the global stability and order of the phase transition of the system by analyzing the Gibbs free energy [71–73,76–79], G, which is defined as

$$G = M - TS. \tag{62}$$

Inserting Equations (21), (24) and (26) in Equation (62), we obtain

$$G = \frac{\left(g^3+r_+^3\right)\left(3(1-a)+8\pi Pr_+^2\right)}{6r_+^2} + \frac{r_+^4\left(a-1-8\pi Pr_+^2\right)+2(1-a)g^3r_+}{4\left(g^3+r_+^3\right)}. \tag{63}$$

The Gibbs free energy for the Hayward–AdS and Schwarzschild–Letelier–AdS solutions are

$$G_H = \frac{(g^3+r_+^3)(3+8\pi P r_+^2)}{6r_+^2} - \frac{r_+^4(1+8\pi P r_+^2)+2g^3 r_+}{4(g^3+r_+^3)}, \quad (64)$$

$$G_L = \frac{1}{12} r_+ \left(3(1-a)+8\pi P r_+^2\right). \quad (65)$$

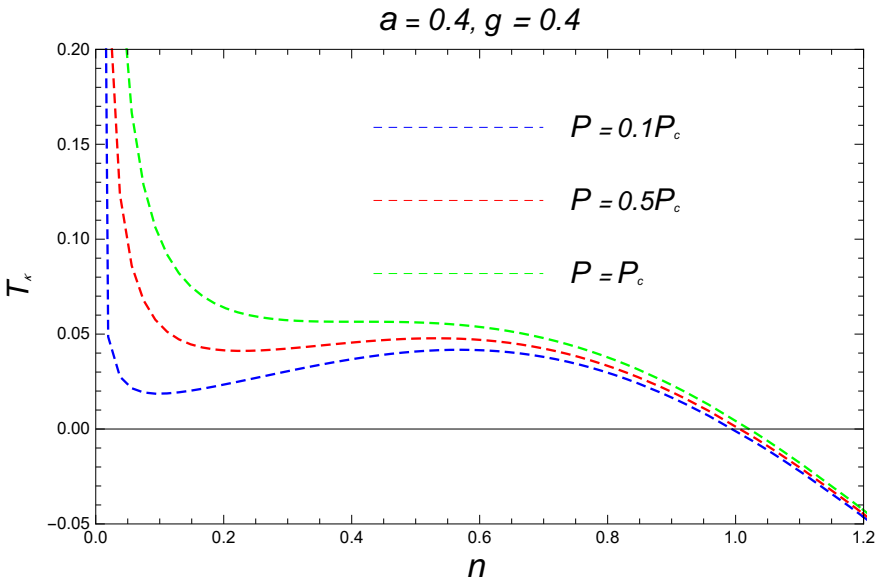

Figure 8. Behavior T_k for Hayward–Schwarzschild–Letelier–AdS solution in terms of number density.

In Figure 9, we show how the Gibbs free energy of the system behaves.

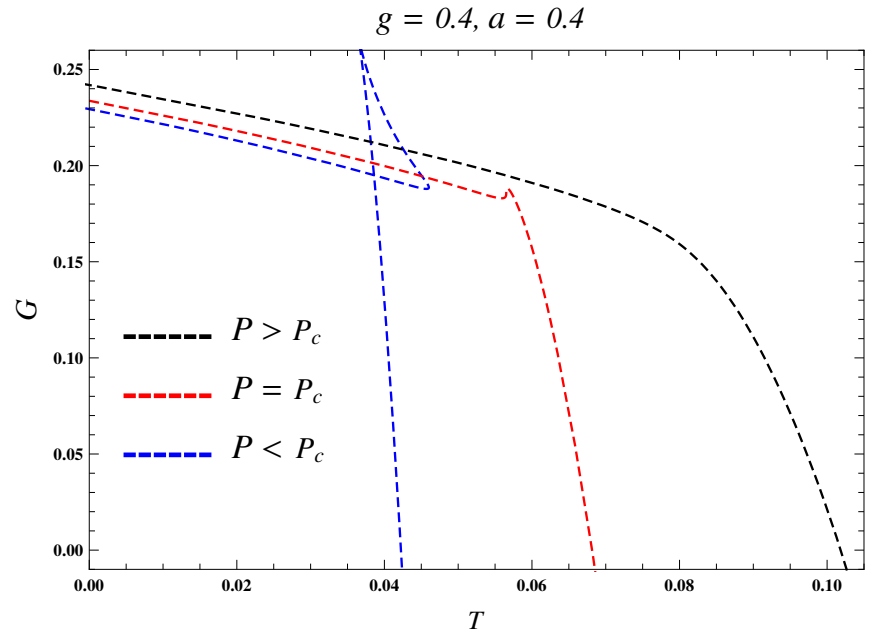

Figure 9. *Cont.*

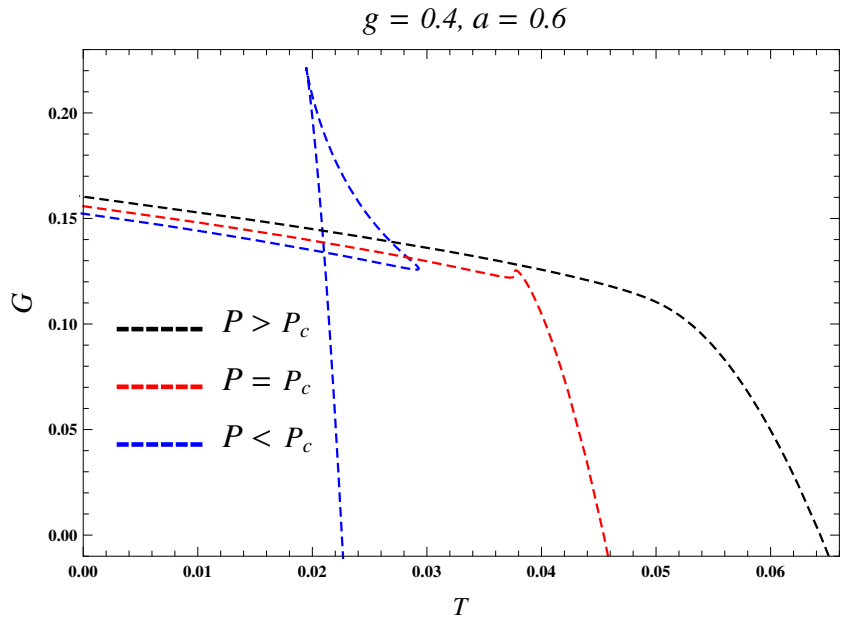

Figure 9. Gibbs free energy for Hayward–Schwarzschild–Letelier–AdS solution as a function of temperature for $P_c = 0.0090686$ (**Top**) and $P_c = 0.0060457$ (**Bottom**).

One can also analyze the phase transition via isothermal compressibility k_T. By using Equations (41) and (48), we obtain

$$k_T = \frac{24\pi r_+^5\left(g^3+r_+^3\right)}{2(1-a)g^6+2g^3r_+^3\left(5(1-a)+16\pi Pr_+^2\right)-r_+^6\left(1-a-8\pi Pr_+^2\right)}. \tag{66}$$

For Hayward–AdS and Schwarzschild–Letelier–AdS, we obtain

$$k_{TH} = \frac{24\pi r_+^5\left(g^3+r_+^3\right)}{2g^6+2g^3r_+^3\left(5+16\pi Pr_+^2\right)-r_+^6\left(1-8\pi Pr_+^2\right)}, \tag{67}$$

$$k_{TL} = -\frac{24\pi r_+^2}{1-a-8\pi Pr_+^2}. \tag{68}$$

Figure 10 shows that small and large BHs with positive isothermal compressibility are thermodynamically stable, whereas, the intermediate BHs are unstable with $k_T < 0$.

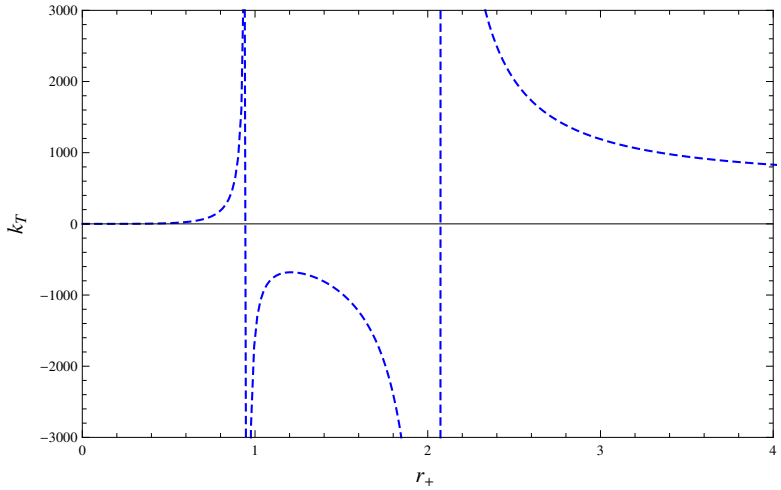

Figure 10. Isothermal compressibility associated with the Hayward–Schwarzschild–Letelier–AdS solution (19) with $g = 0.4$, $p = 0.005$.

5. Critical Exponents

It is important to find out the values of the critical exponents because we can analyze the behavior of thermodynamic quantities like specific heat and isothermal compressibility around the phase transition point, which shows divergence at the transition point. To do so, we use the following expressions [72,73]

$$C_V = T\left(\frac{\partial S}{\partial T}\right) \propto |t|^{-\alpha}, \tag{69}$$

$$\eta = V_1 - V_2 \propto |t|^{\beta}, \tag{70}$$

$$k_T = -\frac{1}{V}\frac{\partial V}{\partial P} \propto |t|^{-\gamma}, \tag{71}$$

$$|P - P_c| \propto |V - V_c|^{\delta}, \tag{72}$$

where η is the difference in volume between the two phases, and $t = T/T_c - 1$. The value of the critical exponent α depends upon the behavior of the specific heat at constant volume. To do so, we rewrite the entropy in terms of volume by using Equations (24) and (47), which yields

$$S(V) = \sqrt[3]{\frac{9V^2\pi}{16}}. \tag{73}$$

Hence, the specific heat at constant volume becomes

$$C_V = T\left(\frac{\partial S}{\partial T}\right)\Big|_V = 0, \tag{74}$$

which signifies $\alpha = 0$. Before going forward, we define some dimensionless quantities as

$$t = \frac{T - T_c}{T_c},\ \omega = \frac{V - V_c}{V_c},\ \text{and}\ p = \frac{P}{P_c}. \tag{75}$$

We use the quantities defined in Equation (75) to write the equation of state (48) as

$$p \approx 1 + t(2.63299 - 0.966326\omega) - 0.0584446\omega^3 + O\left(\omega^4, t\omega^2\right). \tag{76}$$

Using the fact that pressure remains constant during the phase transition, we can write Equation (76) for two different states as

$$1 + t(2.63299 - 0.966326\omega_1) - 0.0584446\omega_1^3 = 1 + t(2.63299 - 0.966326\omega_2) - 0.0584446\omega_2^3, \tag{77}$$

where subscripts 1 and 2 represent the two different states of the BH. By considering t as constant, we can take derivative of p with respect to ω to obtain

$$dp = -\left(0.966326t + 0.1753338\omega^2\right)d\omega. \tag{78}$$

To obtain the critical exponent β, we need to apply the well-known Maxwell's area law, which states [58,72,73,80,81]

$$\int_{\omega_1}^{\omega_2} \omega dp = 0. \tag{79}$$

We solve Equations (77) and (79) to find

$$\omega_1 = -\omega_2 \propto \sqrt{t}\ \text{and}\ \eta \propto \sqrt{t}, \tag{80}$$

which results in $\beta = 1/2$. The critical isotherm can be calculated by taking $t = 0$ as

$$|P - P_c|_{T_c} \propto \omega^3 \propto |V - V_c|^3, \tag{81}$$

and, hence, $\delta = 3$. Now, we use (76) to calculate the isothermal compressibility to obtain

$$k_T \propto \frac{1}{t}, \tag{82}$$

which means $\gamma = 1$. It can be confirmed from the equations below that these critical exponents satisfy the Griffiths, Rushbrooke, and Widom equalities [69,73,82];

$$\alpha + \beta(1+\delta) = 2, \quad \gamma(\delta+1) = (2-\alpha)(\delta-1), \text{ Griffiths} \tag{83}$$

$$\alpha + 2\beta + \gamma = 2, \quad \gamma = \beta(\delta-1), \text{ Widom} \tag{84}$$

which signifies that there are only two independent exponents.

6. Discussion

We began this article by obtaining an exact magnetically charged spherically symmetric Hayward–Letelier AdS BH. The event horizon's structure indicates that the obtained solution may have up to two horizons, depending on the values of the CS parameter a and the magnetic charge g. In the limits, namely $a = 0$ and $g = 0$, the solution reduces to the Hayward–AdS and Schwarzschild–Letelier–AdS BHs, respectively. However, unlike the Hayward BH, the surrounding CS confirmed that our BH solution no longer remains regular.

Furthermore, we analyzed the thermodynamic aspects of the obtained Hayward–Letelier AdS BH solution by investigating various thermodynamic quantities. We started by determining the BH temperature T_κ through its surface gravity and the temperature T_H using the first law of BH thermodynamics. We observe that these two temperatures differ because of the explicit dependence of the NED Lagrangian on the mass M. To address this issue, we revised the first law by introducing a correction factor $W(r_+, g)$ that compensates for changes in the matter sector through fluctuations in the geometry. Additionally, we derived the Smarr formula by utilizing the homogeneity of the BH mass.

Subsequently, we studied the specific heat as a function of entropy and identified regions of thermodynamic stability ($C_P > 0$) as well as thermodynamic instability ($C_P < 0$). We also investigated the critical behavior of the system by obtaining the equation of state and plotting isotherms on the $P - V$ plane. Remarkably, our system exhibits behavior reminiscent of van der Waals fluids for temperatures below the critical temperature. Moreover, we calculated the compressibility factor Z to assess the deviation of the system from an ideal gas. In addition, we analyzed the temperature in terms of the number density of virtual micro-molecules and determined an upper limit on the number density to ensure the physicality of the system ($T_\kappa > 0$).

We employed Gibbs's free energy to explore the system's phase structure. By plotting isobars on the $G - T$ plane, we found that the system can exhibit no phase transition, a first-order phase transition, or a second-order phase transition for $P > P_c$, $P < P_c$, and $P = P_c$, respectively. When $P < P_c$, we observe the existence of small and large stable BH states and intermediate unstable BH states. The small stable BHs undergo a van der Waals-like first-order phase transition to transform into large stable BHs. We also confirmed this phase transition through the behavior of the isothermal compressibility. Furthermore, we analyzed thermodynamic quantities such as specific heat and isothermal quantities near the critical point, which exhibit divergences at critical points. We calculated the critical exponents and found that the system discussed in this article strongly resembles a van der Waals fluid. Notably, only two critical exponents are independent, as presented using the Griffiths, Rushbrooke, and Widom equalities given by Equations (83) and (84).

Author Contributions: Conceptualization, A.K. and S.G.G.; methodology, A.K. and A.S.; software, A.K. and A.S.; validation, A.K., A.S., S.G.G. and A.B.; formal analysis, A.K., A.S., S.G.G. and A.B.; investigation, A.K., A.S., S.G.G. and A.B.; resources, S.G.G.; writing—original draft preparation, A.K. and A.S.; writing—review and editing, A.K., A.S., S.G.G. and A.B.; visualization, A.K., A.S., S.G.G. and A.B.; supervision, S.G.G. and A.B.; project administration, S.G.G. All authors have read and agreed to the published version of the manuscript.

Funding: This research received no external funding.

Institutional Review Board Statement: Not applicable.

Informed Consent Statement: Not applicable.

Data Availability Statement: Not applicable.

Acknowledgments: S.G.G. would like to thank the Inter-University Centre for Astronomy and Astrophysics (IUCAA), Pune for hospitality while this work was being done.

Conflicts of Interest: The authors declare no conflicts of interest.

Abbreviations

The following abbreviations are used in this manuscript:

GR	General Relativity
AdS	Anti-de Sitter
BH	Black Hole
NED	Nonlinear Electrodynamics

References

1. Hawking S.W.; Ellis, G.F.R. *The Large Scale Structure of Spacetime*; Cambridge University Press: Cambridge, UK, 1973.
2. Sakharov, A.D. Nachal'naia stadija rasshirenija Vselennoj i vozniknovenije neodnorodnosti raspredelenija veshchestva. *Sov. J. Exp. Theor. Phys.* **1966**, *22*, 241.
3. Gliner, E.B. Algebraic properties of the energy-momentum tensor and vacuum-like states of matter. *Sov. J. Exp. Theor. Phys.* **1966**, *22*, 378.
4. Bardeen, J. Non-singular general-relativistic gravitational collapse. In Proceedings of the International Conference GR5, Tbilisi, Russia, 9–13 September 1968; p. 174.
5. Ayon-Beato, E.; Garcia, A. The Bardeen model as a nonlinear magnetic monopole. *Phys. Lett. B* **2000**, *493*, 149–152. [CrossRef]
6. Bronnikov, K.A. Comment on Regular black hole in general relativity coupled to nonlinear electrodynamics. *Phys. Rev. Lett.* **2000**, *85*, 4641. [CrossRef]
7. Bronnikov, K.A. Regular magnetic black holes and monopoles from nonlinear electrodynamics. *Phys. Rev. D* **2001**, *63*, 044005. [CrossRef]
8. Ansoldi, S. Spherical black holes with regular center: A Review of existing models including a recent realization with Gaussian sources. *arXiv* **2008**, arXiv:0802.0330.
9. Lemos, J.P.S.; Zanchin, V.T. Regular black holes: Electrically charged solutions, Reissner-Nordström outside a de Sitter core. *Phys. Rev. D* **2011**, *83*, 124005. [CrossRef]
10. Schee, J.; Stuchlik, Z. Gravitational lensing and ghost images in the regular Bardeen no-horizon spacetimes. *J. Cosmol. Astropart. Phys.* **2015**, *6*, 48. [CrossRef]
11. Ali, M.S.; Ghosh, S.G. Exact *d*-dimensional Bardeen-de Sitter black holes and thermodynamics. *Phys. Rev. D* **2018** *98*, 084025. [CrossRef]
12. Kumar, A.; Singh, D.V.; Ghosh, S.G. *D*-dimensional Bardeen-AdS black holes in Einstein–Gauss–Bonnet theory. *Eur. Phys. J. C* **2019**, *79*, 275. [CrossRef]
13. Dymnikova, I. Vacuum nonsingular black hole. *Gen. Relativ. Gravit.* **1992**, *24*, 235–242. [CrossRef]
14. Dymnikova, I. Regular electrically charged structures in nonlinear electrodynamics coupled to general relativity. *Class. Quant. Grav.* **2004**, *21*, 4417–4429. [CrossRef]
15. Xiang, L.; Ling, Y.; Shen, Y.G. Singularities and the Finale of Black Hole Evaporation. *Int. J. Mod. Phys. D* **2013**, *22*, 1342016. [CrossRef]
16. Balart, L.; Vagenas, E.C. Regular black hole metrics and the weak energy condition. *Phys. Lett. B* **2014**, *730*, 14–17. [CrossRef]
17. Balart, L.; Vagenas, E.C. Regular black holes with a nonlinear electrodynamics source. *Phys. Rev. D* **2014**, *90*, 124045. [CrossRef]
18. Neves, J.C.S.; Saa, A. Regular rotating black holes and the weak energy condition. *Phys. Lett. B* **2014**, *734*, 44–48. [CrossRef]
19. Fernando, S. Bardeen?de Sitter black holes. *Int. J. Mod. Phys. D* **2017**, *26*, 1750071. [CrossRef]
20. Hayward, S.A. Formation and evaporation of regular black holes. *Phys. Rev. Lett.* **2006**, *96*, 031103. [CrossRef]

21. Ghosh, S.G.; Kumar, A.; Singh, D.V. Anti-de Sitter Hayward black holes in Einstein–Gauss–Bonnet gravity. *Phys. Dark Univ.* **2020**, *30*, 100660. [CrossRef]
22. Kumar, A.; Singh, D.V.; Ghosh, S.G. Hayward black holes in Einstein–Gauss–Bonnet gravity. *Ann. Phys.* **2020**, *419*, 168214. [CrossRef]
23. Kumar, A.; Baboolal, D.; Ghosh, S.G. Nonsingular black holes in 4D Einstein–Gauss–Bonnet Gravity. *Universe* **2022**, *8*, 244. [CrossRef]
24. Frolov, V.P.; Zelnikov, A. Quantum radiation from an evaporating nonsingular black hole. *Phys. Rev. D* **2017**, *95*, 124028. [CrossRef]
25. Frolov, V.P. Notes on nonsingular models of black holes. *Phys. Rev. D* **2016**, *94*, 104056. [CrossRef]
26. Lin, K.; Li, J.; Yang, S. Quasinormal Modes of Hayward Regular Black Hole. *Int. J. Theor. Phys.* **2013**, *52*, 3771. [CrossRef]
27. Chiba, T.; Kimura, M. A note on geodesics in the Hayward metric. *Prog. Theor. Exp. Phys.* **2017**, *2017*, 043E01. [CrossRef]
28. Mehdipour, S.H.; Ahmadi, M.H. Black Hole Remnants in Hayward Solutions and Noncommutative Effects. *Nucl. Phys. B* **2018**, *926*, 49. [CrossRef]
29. Zhao, S.S.; Xie, Y. Strong deflection gravitational lensing by a modified Hayward black hole. *Eur. Phys. J. C* **2017**, *77*, 272. [CrossRef]
30. Kumar, A.; Ghosh, S.G.; Beesham, A. Extended phase space thermodynamics of Bardeen–Letelier black holes in 4D Einstein–Gauss–Bonnet gravity. *Eur. Phys. J. Plus* **2024**, *139*, 439. [CrossRef]
31. Kumar, A.; Walia, R.K.; Ghosh, S.G. Bardeen Black Holes in the Regularized 4D Einstein–Gauss–Bonnet Gravity. *Universe* **2022**, *8*, 232. [CrossRef]
32. Kumar, A.; Ghosh, S.G.; Wang, A. Effect of dark energy on photon orbits and thermodynamic phase transition for Hayward anti-de Sitter black holes. *Phys. Dark Univ.* **2024**, *46*, 101608. [CrossRef]
33. Maldacena, J.M. The Large N limit of superconformal field theories and supergravity. *Adv. Theor. Math. Phys.* **1998**, *2*, 231–252. [CrossRef]
34. Gubser, S.S.; Klebanov, I.R.; Polyakov, A.M. Gauge theory correlators from noncritical string theory. *Phys. Lett. B* **1998**, *428*, 105–114. [CrossRef]
35. Witten, E. Anti-de Sitter space and holography. *Adv. Theor. Math. Phys.* **1998**, *2*, 253–291. [CrossRef]
36. Hawking, S.W. Particle Creation by black holes. *Commun. Math. Phys.* **1975**, *43*, 199. [CrossRef]
37. Bekenstein, J.D. Black holes and entropy. *Phys. Rev. D* **1973**, *7*, 2333–2346. [CrossRef]
38. Bardeen, J.M.; Carter, B.; Hawking, S.W. The Four laws of black hole mechanics. *Commun. Math. Phys.* **1973**, *31*, 161–170. [CrossRef]
39. Hawking, S.W.; Page, D.N. Thermodynamics of black holes in anti-De Sitter Space. *Commun. Math. Phys.* **1983**, *87*, 577. [CrossRef]
40. Kastor, D.; Ray, S.; Traschen, J. Enthalpy and the Mechanics of AdS black holes. *Class. Quantum Gravity* **2009**, *26*, 195011. [CrossRef]
41. Dolan, B.P. Pressure and volume in the first law of black hole thermodynamics. *Class. Quantum Gravity* **2011**, *28*, 235017. [CrossRef]
42. Gunasekaran, S.; Mann, R.B.; Kubiznak, D. Extended phase space thermodynamics for charged and rotating black holes and Born-Infeld vacuum polarization. *J. High Energy Phys.* **2012**, *11*, 110. [CrossRef]
43. Kubiznak, D.; Mann, R.B. P-V criticality of charged AdS black holes. *J. High Energy Phys.* **2012**, *7*, 33. [CrossRef]
44. Kubiznak, D.; Mann, R.B.; Teo, M. Black hole chemistry: Thermodynamics with Lambda. *Class. Quantum Gravity* **2017**, *34*, 063001. [CrossRef]
45. Altamirano, N.; Kubiznak, D.; Mann, R.B. Reentrant phase transitions in rotating anti–de Sitter black holes. *Phys. Rev. D* **2013**, *88*, 101502. [CrossRef]
46. Altamirano, N.; Kubizňák, D.; Mann, R.B.; Sherkatghanad, Z. Kerr-AdS analogue of triple point and solid/liquid/gas phase transition. *Class. Quantum Gravity* **2014**, *31*, 042001. [CrossRef]
47. Johnson, C.V. Holographic Heat Engines. *Class. Quantum Gravity* **2014**, *31*, 205002. [CrossRef]
48. Synge, J.L. *Relativity: The General Theory*; North Holland: Amsterdam, The Netherlands, 1966; p. 175.
49. Letelier, P.S. Clouds of Strings in General Relativity. *Phys. Rev. D* **1979**, *20*, 1294. [CrossRef]
50. Graça, J.P.M.; Lobo, I.P.; Bezerra, V.B.; Moradpour, H. Effects of a string cloud on the criticality and efficiency of AdS black holes as heat engines. *Eur. Phys. J. C* **2018**, *78*, 823. [CrossRef]
51. Lee, T.H.; Ghosh, S.G.; Maharaj, S.D.; Baboolal, D. Lovelock black hole thermodynamics in a string cloud model. *arXiv* **2015**, arXiv:1511.03976.
52. Lee, T.H.; Baboolal, D.; Ghosh, S.G. Lovelock black holes in a string cloud background. *Eur. Phys. J. C* **2015**, *75*, 297. [CrossRef]
53. Herscovich, E.; Richarte, M.G. Black holes in Einstein–Gauss–Bonnet gravity with a string cloud background. *Phys. Lett. B* **2010**, *689*, 192–200. [CrossRef]
54. Ghosh, S.G.; Papnoi, U.; Maharaj, S.D. Cloud of strings in third order Lovelock gravity. *Phys. Rev. D* **2014**, *90*, 044068. [CrossRef]
55. Ghosh, S.G.; Maharaj, S.D. Cloud of strings for radiating black holes in Lovelock gravity. *Phys. Rev. D* **2014**, *89*, 084027. [CrossRef]
56. Singh, D.V.; Ghosh, S.G.; Maharaj, S.D. Clouds of strings in 4*D* Einstein–Gauss–Bonnet black holes. *Phys. Dark Univ.* **2020**, *30*, 100730. [CrossRef]
57. Plebanski, J.; Krasinski, A. *An Introduction to General Relativity and Cosmology*; Cambridge University Press: New York, NY, USA, 2006.
58. Sood, A.; Kumar, A.; Singh, J.K.; Ghosh, S.G. Thermodynamic stability and *P–V* criticality of nonsingular-AdS black holes endowed with clouds of strings. *Eur. Phys. J. C* **2022**, *82*, 227. [CrossRef]

59. Ruffini, R.; Wheeler, J.A. Introducing the black hole. *Phys. Today* **1971**, *24*, 30. [CrossRef]
60. Misner, C.W.; Thorne, K.S.; Wheeler, J.A. *Gravitation*; W. H. Freeman: San Francisco, CA, USA, 1973; ISBN 978-0-7167-0344-0/978-0-691-17779-3.
61. Bekenstein, J.D. Black holes and the second law. *Lett. Nuovo C.* **1972**, *4*, 737–740. [CrossRef]
62. Wald, R.M. The thermodynamics of black holes. *Living Rev. Relativ.* **2001**, *4*, 6. [CrossRef]
63. Ma, M.S.; Zhao, R. Corrected form of the first law of thermodynamics for regular black holes. *Class. Quantum Gravity* **2014**, *31*, 245014. [CrossRef]
64. Zhang, Y.; Gao, S. First law and Smarr formula of black hole mechanics in nonlinear gauge theories. *Class. Quantum Gravity* **2018**, *35*, 145007. [CrossRef]
65. Maluf, R.V.; Neves, J.C.S. Thermodynamics of a class of regular black holes with a generalized uncertainty principle. *Phys. Rev. D* **2018**, *97*, 104015. [CrossRef]
66. Rodrigues, M.E.; Silva, M.V.d.; Vieira, H.A. Bardeen-Kiselev black hole with a cosmological constant. *Phys. Rev. D* **2022**, *105*, 084043. [CrossRef]
67. Singh, D.V.; Siwach, S. Thermodynamics and P-v criticality of Bardeen-AdS black hole in 4*D* Einstein–Gauss–Bonnet Gravity. *Phys. Lett. B* **2020**, *808*, 135658. [CrossRef]
68. Hankey, A.; Stanley, H.E. Systematic Application of Generalized Homogeneous Functions to Static Scaling, Dynamic Scaling, and Universality. *Phys. Rev. B* **1972**, *6*, 3515. [CrossRef]
69. Stanley, H.E. *Introduction to Phase Transitions and Critical Phenomena*; Oxford University Press: London, UK, 1971.
70. Davies, P.C.W. Thermodynamics of black holes. *Proc. R. Soc. Lond. A* **1977**, *353*, 499–521. [CrossRef]
71. Dehyadegari, A.; Sheykhi, A.; Montakhab, A. Novel phase transition in charged dilaton black holes. *Phys. Rev. D* **2017**, *96*, 084012. [CrossRef]
72. Dayyani, Z.; Sheykhi, A.; Dehghani, M.H.; Hajkhalili, S. Critical behavior and phase transition of dilaton black holes with nonlinear electrodynamics. *Eur. Phys. J. C* **2018**, *78*, 152. [CrossRef]
73. Wei, S.W.; Liu, Y.X. Extended thermodynamics and microstructures of four-dimensional charged Gauss–Bonnet black hole in AdS space. *Phys. Rev. D* **2020**, *101*, 104018. [CrossRef]
74. Gallagher, J.E. *Natural Gas Measurement Handbook*; Gulf Publishing Company: Huston, TX, USA, 2006.
75. Wei, S.W.; Liu, Y.X. Insight into the Microscopic Structure of an AdS black hole from a Thermodynamical Phase Transition. *Phys. Rev. Lett.* **2015**, *115*, 111302; Erratum in *Phys. Rev. Lett.* **2016** *116*, 169903. [CrossRef] [PubMed]
76. Liu, Y.; Zou, D.C.; Wang, B. Signature of the Van der Waals like small-large charged AdS black hole phase transition in quasinormal modes. *J. High Energy Phys.* **2014**, *9*, 179. [CrossRef]
77. Nam, C.H. Non-linear charged dS black hole and its thermodynamics and phase transitions. *Eur. Phys. J. C* **2018**, *78*, 418. [CrossRef]
78. Dehyadegari, A.; Sheykhi, A. Critical behavior of charged dilaton black holes in AdS space. *Phys. Rev. D* **2020**, *102*, 064021. [CrossRef]
79. Kumara, A.N.; Rizwan, C.L.A.; Hegde, K.; Ali, M.S.; Ajith, K.M. Ruppeiner geometry, reentrant phase transition, and microstructure of Born-Infeld AdS black hole. *Phys. Rev. D* **2021**, *103*, 044025. [CrossRef]
80. Kumar, A.; Ghosh, S.G.; Maharaj, S.D. Nonsingular black hole chemistry. *Phys. Dark Univ.* **2020**, *30*, 100634. [CrossRef]
81. Kumar, A.; Ghosh, S.G. Nonsingular black hole chemistry in 4D Einstein–Gauss–Bonnet gravity. *Nucl. Phys. B* **2023**, *987*, 116089. [CrossRef]
82. Griffiths, R.B. Ferromagnets and Simple Fluids near the Critical Point: Some Thermodynamic Inequalities. *J. Chem. Phys.* **1965**, *43*, 1958. [CrossRef]